CHIN. PHYS. LETT. Vol. 33, No. 4 (2016) 040601

An Accurate Frequency Control Method and Atomic Clock Based on Coherent Population Beating Phenomenon

Yu-Xin Zhuang(庄煜昕), Dai-Ting Shi(石岱庭), Da-Wei Li(李大为), Yi-Gen Wang(王乙亘), Xiao-Na Zhao(赵晓娜), Jian-Ye Zhao(赵建业), Zhong Wang(汪中)**

School of Electronics Engineering and Computer Science, Peking University, Beijing 100871

(Received 30 November 2015)

An accurate frequency control method and atomic clock based on the coherent population beating (CPB) phenomenon is implemented. In this scheme, the frequency difference of an rf and an atomic transition frequency can be digitally obtained by measuring the CPB oscillation frequency. The frequency measurement resolution of several milli-hertz can be achieved by using a 10 MHz oven controlled crystal oscillator as the reference. The expression of the Allan deviation of the CPB clock is theoretically deduced and it is revealed that the Allan deviation is inversely proportional to the signal-to-noise ratio and proportional to the line-width of coherent population trapping spectrum. We also approve that the CPB atomic clock has a large toleration of the drift of the local oscillator. In our CPB experimental system, a frequency instability of 3.0×10^{-12} *at 1000 s is observed. The important feature of high frequency measurement resolution of the CPB method may also be used in magnetometers, atomic spectroscopy, and other related research.*

PACS: 06.30.Ft, 95.55.Sh, 42.50.Gy DOI: 10.1088/0256-307X/33/4/040601

The coherent population beating (CPB) phenomenon has been observed and studied by various research groups[1–4] for a long time. This phenomenon was seen as the transient oscillation of coherent population trapping (CPT),[5–7] which is caused by Raman detuning. The CPB phenomenon can be observed in a Λ-type three-level system where two near-resonance coherent light fields are applied to an atomic ensemble. Initially the frequency difference of the two laser fields $\omega = \omega_a - \omega_b$ equals to the ground state hyperfine splitting frequency ω_{21} so that the atoms are trapped in the CPT dark state. If ω is suddenly detuned from ω_{21} by δ, atoms will experience a temporal evolution to exit the dark state. The evolution of the excited state population ρ_{33} can be deduced by solving the quantum Liouville equation[4]

$$\rho_{33} = A - Ce^{-(\gamma_2 + \frac{\Omega^2}{\Gamma})t}\cos(\delta t + \varepsilon), \qquad (1)$$

where A, C and ε are coefficients, A represents the steady-state solution, and C represents the amplitude of the transient oscillation respectively. Since the frequency of the transient oscillation described in Eq. (1) is equal to δ, the beat frequency of ω and ω_{21}, we call it coherent population beating. The amplitude of CPB oscillation decays at the rate of $\gamma_2 + \Omega^2/\Gamma$, which means that the frequency spectrum of CPB oscillation has the same line-width as CPT.[8]

We previously proposed that the CPB effect can be used to achieve an atomic clock.[8,9] In this study, we demonstrate an experimental implementation of the CPB atomic clock using the method of high resolution frequency measurement. We also prove that the CPB atomic clock has the potentials of high frequency discrimination ability and high frequency stability.

The experimental setup of our CPB atomic clock is shown in Fig. 1(a).

The physical part includes a cylindrical ^{87}Rb vapor, a half wave plate ($\lambda/2$), a polarization splitting prism (PBS) and a quarter wave plate ($\lambda/4$). The cell is 5 cm in length and 2.5 cm in diameter, filled with buffer gas Ar and Ne. The cell is magnetic shielded and works at room temperature. An axial magnetic field B_z is applied to distinguish different Zeeman sublevels. The two ground states $|^2S_{1/2}, F = 1, M_F = 0\rangle$ and $|^2S_{1/2}, F = 2, M_F = 0\rangle$ are coupled to each other via a common excited state $|^2P_{1/2}, F' = 1, 2, M'_F = 1\rangle$ by using two σ^+ lights. The driven current of a 795 nm vertical cavity surface emitting laser (VCSEL) is modulated by an $\omega/2$ (approximately 3.4 GHz) rf signal to generate multi-sidebands. The $+1$ and -1 sidebands are used for CPB signal excitation. To periodically excite CPB oscillation, the frequency of the rf signal is modulated by a 60 Hz square wave to make ω alternate between ω_{21} and $\omega_{21}+\delta$. Under our experimental condition, the amplitude of CPB oscillation decays to the magnitude of noise in several milliseconds. Here δ is set to be at $+3$ kHz, a value that can ensure enough oscillation periods in one excitation of CPB. Figure 1(b) shows the CPB signal which is obtained by detecting the intensity of the light transmitted through the Rb cell.

A reshaping circuit converts the decaying CPB signal to a square wave signal with a uniform amplitude and with the same frequency as CPB ($f_x = \delta$). Signal f_x is then sent to a field programmable gate array (FPGA) for frequency measurement. FPGA also controls the frequency tuning word (K) of a direct digital synthesizer (DDS). The output 10 MHz standard signal f_{out} of the CPB clock is generated by this DDS.

**Corresponding author. Email: zw@pku.edu.cn

© 2016 Chinese Physical Society and IOP Publishing Ltd

The frequency synthesizer, FPGA and DDS share the same 10 MHz (f_s) signal generated by an oven controlled crystal oscillator (OCXO) as reference. The relationship between f_{out} and δ is

$$f_{out} = \frac{K}{2^{48}} f_{clk} = \frac{K}{2^{48}} \left(f_{clk0} + \frac{\delta - 3000\,\text{Hz}}{34.17} \right), \quad (2)$$

where f_{clk} is the clock frequency of DDS, $f_{clk} = 20 f_s = 200$ MHz, and f_{clk} takes into account of the frequency drift of f_s while f_{clk0} does not. Suppose that there is a frequency drift df_s of the 10 MHz (f_s) signal, the frequency synthesizer output $\omega/2$ will proportionally shift $341.7df_s$, which will shift the CPB frequency δ by $683.4df_s$. For example, if the 10 MHz signal from the OCXO shifts $df_s = 0.01$ Hz, the frequency synthesizer output $\omega/2$ will shift 3.4 Hz proportionally, and then the obtained CPB oscillation frequency will change 6.8 Hz. The DDS clock frequency shifts $20df_s$. With the above relations, the actual DDS clock frequency f_{clk} can be deduced. Let the left side of Eq. (2) equal exactly to 10 MHz, then the frequency tuning word K can be calculated for every measured CPB frequency value δ around 3 kHz. FPGA measures the frequency drift of δ and correspondingly changes K to compensate for the frequency drift of the DDS clock frequency in every 1 s. In this method, the output 10 MHz signal f_{out} is referenced to the ^{87}Rb ground-state hyperfine splitting frequency ω_{21}. The resolution of frequency tuning word is $1/2^{48}$, which is at the magnitude of 3×10^{-15}.

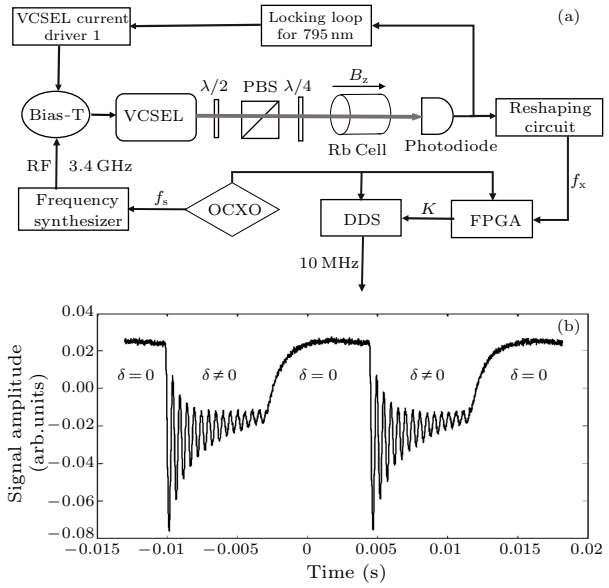

Fig. 1. The block diagram of the CPB atomic clock. VCSEL is a vertical cavity surface emitting laser; PBS is a polarization splitting prism; $\lambda/2$ is a half wave plate; $\lambda/4$ is a quarter wave plate; OCXO is an oven controlled crystal oscillator; FPGA is a field programmable gate array; DDS is a direct digital synthesizer; and K is the frequency control word of DDS. (b) The CPB oscillation signal detected by the photodiode.[9]

One advantage of the CPB clock is that the locking loop can be removed and the risk of losing lock is avoided. To establish the coherence of atoms and then to excite CPB oscillation, we do not need ω to be exactly equal to ω_{21}. We have carried out simulations for ρ_{33} under different detuning conditions using the quantum Liouville equation.[4] The results are shown in Fig. 2. The parameter $\gamma_2 + \Omega^2/\Gamma$ is set as 500 Hz. Let ω be expressed as $\omega_{21} + \delta$. In the first 10 ms, which is the CPT preparation stage, δ equals to 0 Hz, 80 Hz, 150 Hz, 300 Hz in Figs. 2(a)–2(d), respectively. In the second 10 ms, which is the CPB oscillation stage, δ equals 3 kHz plus the detuning in the first stage.

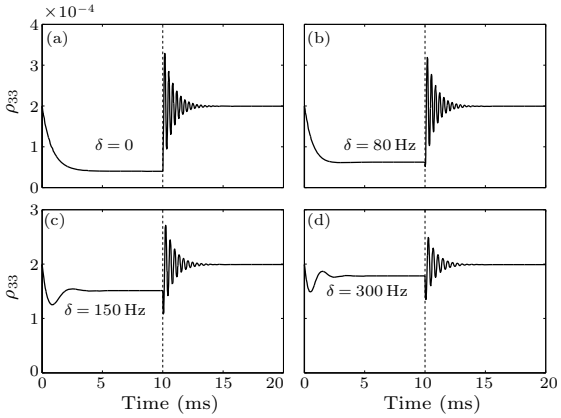

Fig. 2. The simulation results for ρ_{33} under different detunings. The parameter $\gamma_2 + \Omega^2/\Gamma$ is set as 500 Hz. The first 10 ms is the CPT preparation stage and the second 10 ms is the CPB excitation stage. The Raman detuning equals δ in the first 10 ms and 3 kHz+δ in the second 10 ms.

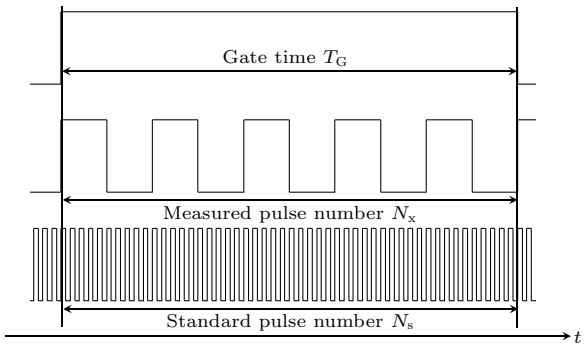

Fig. 3. The schematic diagram of the frequency counting method.

It can be seen that the CPB oscillation can still be excited if there is a detuning in the CPT preparation stage, only the amplitude will be smaller. In our experimental conditions, the full width at half maximum of CPT is less than 300 Hz. We have even observed a CPB oscillation excited by the CPT preparation of 1.2 kHz detuning, which is far outside CPT line-width. The amplitude of this CPB signal is reduced to 1/9 of the CPB signal excited by zero detuning CPT preparation. However, as long as the amplitude of CPB signal exceeds the noise, CPB signal can be converted correctly by the reshaping circuit and CPB frequency can be measured normally. This enables the CPB clock to

have a large toleration of the drift of the local oscillator.

The CPB method also has a high frequency discrimination ability, which does a subtraction that converts the absolute frequency drift of a high frequency signal to the absolute drift of a low frequency signal. Since this low frequency signal δ is about 3 kHz, its drift can be measured with sufficiently high resolution by using the 10 MHz signal of OCXO as a reference. The principle of the high resolution frequency measurement method is illustrated in Fig. 3.

During the measurement gate time $T_{\rm G}$, the pulses number $N_{\rm x}$ of the measured square wave signal ($f_{\rm x} = \delta$) and the pulses number $N_{\rm s}$ of the standard square wave signal ($f_{\rm s}$) are counted. $N_{\rm x}$ and $N_{\rm s}$ satisfies the following relationship:

$$T_{\rm G} = N_{\rm s}/f_{\rm s} = N_{\rm x}/f_{\rm x}. \tag{3}$$

From Eq. (3), $f_{\rm x}$ can be calculated. The opening and closing of the measurement gates are triggered by the rising edge of the measured signal ($f_{\rm x}$) to ensure that one $T_{\rm G}$ region always includes complete periods of the signal $f_{\rm x}$, which eliminates ±1 counting errors of $N_{\rm x}$.[10] The relative measurement uncertainty of $f_{\rm x}$ during one $T_{\rm G}$ time is

$$\frac{df_{\rm x}}{f_{\rm x}} = \frac{dN_{\rm s}}{N_{\rm s}} + \frac{df_{\rm s}}{f_{\rm s}}. \tag{4}$$

The counting uncertainty $dN_{\rm s}$ can be as small as ±1. However, $dN_{\rm s}$ will be larger if the rising edge slope of the signal $f_{\rm x}$ and its noise are taken into consideration. Here $N_{\rm s}$ is limited by $T_{\rm G}$, and $T_{\rm G}$ is limited by the signal-to-noise ratio and the decay rate of CPB oscillation signal. Let S be the initial amplitude of CPB, N be the noise amplitude, S/N be the signal-to-noise ratio, then $T_{\rm G}$ satisfies the relationship $S\exp\{-T_{\rm G}(\gamma_2 + \Omega^2/\Gamma)\} \approx N$, thus

$$T_{\rm G} \approx \frac{\ln(S/N)}{(\gamma_2 + \Omega^2/\Gamma)}. \tag{5}$$

Under our experimental conditions, $T_{\rm G}$ is several milliseconds and the pulses numbers of $N_{\rm x}$ is about 20, which means that $N_{\rm s}$ is about 67000. Assuming that $dN_{\rm x} = 1$, $df_{\rm s}/f_{\rm s}$ of the OCXO is about 3×10^{-11}, which is much smaller than the first term in Eq. (5) and can be ignored. Then $df_{\rm x}/f_{\rm x}$ is estimated to be 1.4×10^{-5}. The frequency measurement and compensation period is 1 s. In 1 s CPB oscillation is excited repeatedly for 60 times. Here $f_{\rm x}$ is measured for 60 times to achieve an average value, so $df_{\rm x}/f_{\rm x}$ can be reduced to $1/\sqrt{60}$, which is 2×10^{-6}. The frequency measurement resolution $df_{\rm x}$ can be less than 6 mHz. According to Eq. (4), the measurement resolution $df_{\rm x}$ can still be improved by using a reference with higher frequency and higher frequency stability and by optimizing the digital signal processing.

The fluctuation of clock output frequency $df_{\rm out}$ in i+1 s is decided by the measurement uncertainty $df_{\rm x}$ in i s and the fluctuation of OCXO $df_{\rm s}$ in i+1 s. If $df_{\rm s}$ is ignored, the limitation performance of the CPB atomic clock can be analyzed. According to Eq. (2), we have

$$df_{\rm out} = 10\,{\rm MHz} \times \frac{df_{\rm x}}{6.834\,{\rm GHz}}. \tag{6}$$

Then we can obtain the Allan deviation $\sigma_{\rm y}$ at 1 s caused by the CPB frequency measurement uncertainty, which is better than 9×10^{-13} theoretically. Using Eqs. (3)–(6), $\sigma_{\rm y}$ can also be expressed as

$$\begin{aligned}\sigma_{\rm y}(\tau = 1{\rm s}) &\approx \frac{df_{\rm out}}{10\,{\rm MHz}} \approx \frac{df_{\rm x}}{6.8\,{\rm GHz}} \approx \frac{f_{\rm x}}{\nu_0}\frac{1}{N_{\rm s}}\sqrt{\frac{T_{\rm c}}{\tau}} \\ &\approx \frac{f_{\rm x}}{\nu_0}\frac{1}{T_{\rm G}f_{\rm s}}\sqrt{\frac{T_{\rm c}}{\tau}} = \alpha\frac{1}{\nu_0 T_{\rm G}}\sqrt{\frac{T_{\rm c}}{\tau}} \\ &\approx \alpha\frac{1}{\nu_0}\frac{(\gamma_2 + \Omega^2/\Omega)}{\ln(S/N)}\sqrt{\frac{T_{\rm c}}{\tau}} \\ &= \alpha\frac{\Delta\nu/\nu_0}{\ln(S/N)}\sqrt{\frac{T_{\rm c}}{\tau}},\end{aligned} \tag{7}$$

where α is a constant coefficient, $T_{\rm c}$ is the period of one CPT-CPB excitation cycle, and $\Delta\nu$ is the line-width of CPT, which is equal to $\gamma_2 + \Omega^2/\Gamma$. It is noteworthy that Eq. (7) is quite similar to $\sigma_{\rm y}$ of conventional passive atomic clocks.[11] A narrower line-width and a better S/N ratio will contribute to a lower $\sigma_{\rm y}$.

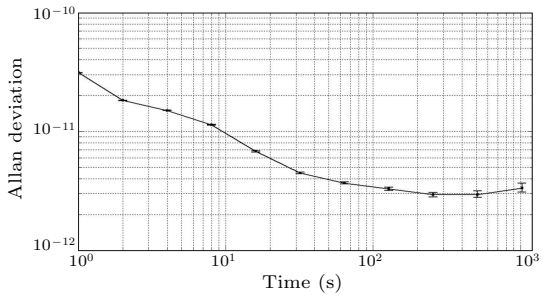

Fig. 4. The frequency instability of the output frequency of the CPB atomic clock. The horizontal axis stands for the integral time of frequency measurement. The error bar in each data point represents the confidence intervals of the Allan deviations.

The frequency instability of our table experimental system of CPB atomic clock has been measured, as shown in Fig. 4. The Allan deviation $\sigma_{\rm y}$ is about 3.2×10^{-11} at 1 s and 3.3×10^{-12} at 1000 s. The error bars represent the confidence intervals of the Allan deviations. In the sampling time (τ) range within 256 s, Allan deviation approximately decreases at the rate of $3.29\times10^{-11}\tau^{-1/2}$, which indicates that the white frequency noise is dominant in the short term.

The measured Allan deviation at 1 s is not as good as $\sigma_{\rm y}$ calculated by Eq. (7). The possible reason is that during two frequency compensations, the output frequency fluctuation is mainly decided by OCXO and the phase noise of DDS. Without the frequency compensation of FPGA, the output frequency instability

of the DDS which is referenced to the OCXO is measured as 3×10^{-11} at 1 s. Equation (7) estimates the limitation performance of the CPB method and does not take into account the fluctuation of OCXO. With a better local oscillation and a reduction of DDS phase noise, the CPB clock may tend to achieve its limitation.

In conclusion, we have demonstrated that the CPB phenomenon can be effectively used to achieve an atomic frequency standard. The frequency drift of local oscillator in the clock can be quantitatively obtained by measuring the drift of CPB frequency through the digital processing method. The CPB method eliminates the possibility of clock frequency losing lock, and can even measure and compensate for a drift of rf frequency outside the CPT line-width. The measurement resolution of CPB frequency is about 6 mHz, which can still be further improved by using reference with higher frequency and higher frequency stability. In the experimental system, the frequency instabilities 3.2×10^{-11} at 1 s and 3.0×10^{-12} at 1000 s are observed. The high frequency measurement resolution of the CPB method may also be used in magnetometers, atomic spectroscopy, and other related research.

References

[1] Park S J, Cho H, Kwon T Y and Lee H S 2004 *Phys. Rev.* A **69** 023806
[2] Gu S H and Behr J A 2003 *Phys. Rev.* A **68** 015804
[3] Valente P, Failache H and Lezama A 2002 *Phys. Rev.* A **65** 023814
[4] Meinert F, Basler C, Lambrecht A, Welte S and Helm H 2012 *Phys. Rev.* A **85** 013820
[5] Alzetta G, Gozzini A, Moi L and Orriols G 1976 *Il Nuovo Cimento* B **36** 5
[6] Wang Z 2014 *Chin. Phys.* B **23** 030601
[7] Vanier J 2005 *Appl. Phys.* B **81** 421
[8] Guo T, Deng K, Chen X Z and Wang Z 2009 *Appl. Phys. Lett.* **94** 151108
[9] Li D W, Shi D T, Hu E M, W Y G, Tian L, Zhao J Y and Wang Z 2014 *Appl. Phys. Express* **7** 112203
[10] Fang Y and Chen X 2012 *Engineering* **4** 696
[11] Bauch A and Telle H R 2002 *Rep. Prog. Phys.* **65** 789